

# Exact Spectral Function of One-Dimensional Bose Gases

Song Cheng,<sup>1</sup> Yang-Yang Chen,<sup>2,3,\*</sup> Xi-Wen Guan,<sup>4,5,6</sup> Wen-Li Yang,<sup>2,3,6</sup> Rubem Mondaini,<sup>1</sup> and Hai-Qing Lin<sup>1,7,†</sup>

<sup>1</sup>Beijing Computational Science Research Center, Beijing 100193, China

<sup>2</sup>Shaanxi Key Laboratory for Theoretical Physics Frontiers, Xi'an 710069, China

<sup>3</sup>Institute of Modern Physics, Northwest University, Xi'an 710069, China

<sup>4</sup>State Key Laboratory of Magnetic Resonance and Atomic and Molecular Physics, Wuhan Institute of Physics and Mathematics, Chinese Academy of Sciences, Wuhan 430071, China

<sup>5</sup>Department of Theoretical Physics, Research School of Physics and Engineering, Australian National University, Canberra ACT 0200, Australia

<sup>6</sup>Peng Huanwu Center for Fundamental Theory, Xi'an 710069, China

<sup>7</sup>Department of Physics, Beijing Normal University, Beijing 100875, China

(Dated: October 3, 2022)

Strong correlation in one-dimensional (1D) quantum systems drastically changes their dynamic and transport properties in the presence of the interaction. In this letter, combining quantum integrable theory with numerics, we exactly compute the spectral function of 1D Lieb-Liniger gas at a many-body level of large scales. It turns out that a full capture of the power-law singularities in the vicinities of thresholds requires system size as large as thousands of particles. Our research essentially confirms the validity of the nonlinear Tomonaga-Luttinger liquid and provides a reliable technique for studying critical behaviour emerged only in thermodynamic limit.

PACS numbers: 03.75.Kk, 05.30.Jp

*Introduction* — For interacting particles in one dimension (1D), reducing dimensionality inevitably reinforces the quantum correlation in comparison with their higher dimensional counterparts [1]. An immediate consequence is that Fermi liquid theory [2, 3] based on quasi-particle pictures fails to describe the low energy physics of 1D systems. The role of quasi-particle excitation is taken over by collective excitation in 1D [4] and alternative theoretic tools responsible for that are bosonization and Tomonaga-Luttinger liquid (TLL) theory [1, 5]. The strong correlation in 1D blurs the distinction between microscopic constituents, namely bosons and fermions [6–8]. Hence, study on interacting bosons in 1D is of particular importance for revealing the characteristic of strongly correlated systems as well as benchmark many-body phenomena in 1D and higher dimensions, such as quantum criticality [9–11], Mott phase transition [1, 12], power-law singularities on the spectral thresholds [5, 13–19] etc.

The past few decades have witnessed explosive developments in ultracold-atom manipulation and control. Various correlation functions in 1D quantum systems have been measured including momentum distribution via optical imaging [10, 20], spectral function via photoemission spectroscopy [21] and momentum-resolved Raman spectroscopy [22], dynamical structure factor (DSF) via Bragg scattering spectroscopy [23–25] etc. On the other hand, much theoretical effort has been made in computing dynamical response functions [26–31], DSF [24, 32], spectral function (SF) [33, 34] and many-body local and nonlocal multi-particle correlations [35–40]. In this scenario, the TLL provides qualitative predictions for momentum distribution, density-density correlation, one-body reduced density matrix [1, 6, 41] etc. In particular, the Nonlinear TLL, involving the nonlinear effects

of dispersion relation, has been used to study the Fermi edge singularity (FES) of Lieb-Liniger model [13].

The Lieb-Liniger gas [42] is a prototypical exactly solvable model, see reviews [6, 43–46]. Based on exactly solution of this model, the space-, time- and temperature-dependent correlation functions can be derived in terms of Fredholm determinants, where each Fredholm operator further relates to the special Riemann problem [47–50]. The quantum integrability also enables a disparate access to correlation properties in terms of evaluating the form factors for a finite system [45, 48, 51–53]. Following this approach the DSF [54, 55] and one-body dynamical correlation functions [56, 57] have been studied in detail. Nevertheless, the singular behaviour of the SF and DSF still imposes a big theoretical challenge in 1D systems.

The SF represents the probability of tunneling a boson with specified momentum and energy, showing the FES in both particle and hole excitations. In this Letter, we exactly calculate SF of the Lieb-Liniger model by combining form factor with numerics at full momentum and energy scales. The intermediate interaction strength is considered in particular, which is ubiquitous in experiments but hard to deal with in theories. By virtue of our algorithm, the full picture of SF of arbitrary interaction strength is obtained, in particular a typical line shape of the SF for the system size as large as  $N = 4000$ . The edge exponents of the SF in the vicinities of the thresholds essentially confirm the nonlinear TLL. Our method provides a versatile playground for obtaining dynamical correlated properties in 1D, as a benchmark in both theoretical and experimental aspects.

*Method* — The Lieb-Liniger model describes  $N$  bosons

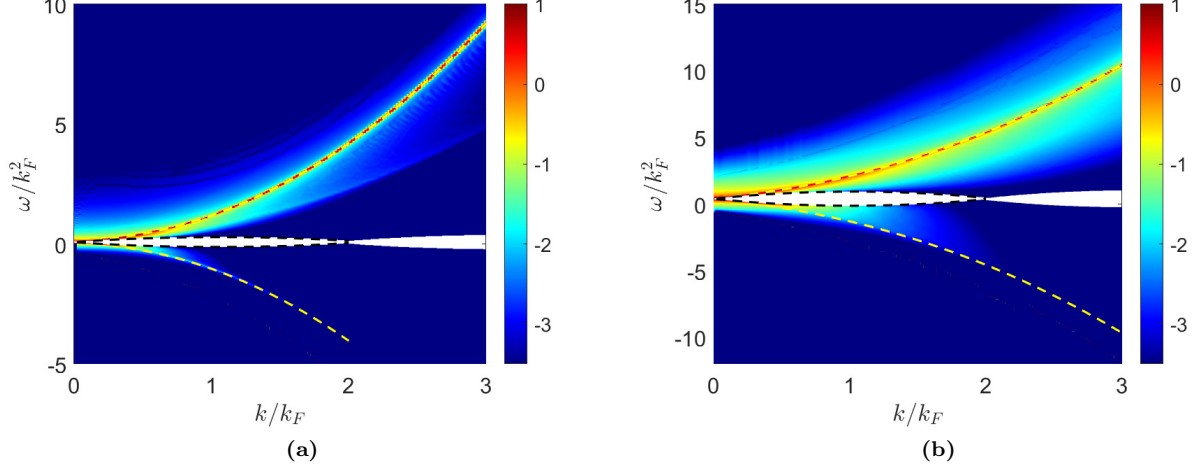


FIG. 1: The momentum-energy resolved SF of Lieb-Liniger gas in ground state of system with  $N = L = 100$ . The subfigures (a) and (b) are for interaction strength  $\gamma = 0.5$  and  $4.0$  respectively with sum rules  $0.9999$  and  $0.9935$ . Momentum and energy are given in the units of Fermi energy and Fermi momentum respectively. For clarity we adopt logarithm of SF, and the higher the value the brighter the color. Note that the blank region indicates SF is not applicable due to no states therein. The yellow (black) dashed lines are the Lieb - I (- II) dispersion relations.

confined on a line of length  $L$  with contact interaction

$$H = -\sum_{i=1}^N \frac{\partial^2}{\partial x_i^2} + 2c \sum_{i>j}^N \delta(x_i - x_j) \quad (1)$$

where  $c > 0$  ( $c < 0$ ) stands for repulsion (attraction), and a dimensionless parameter  $\gamma = c * L / N$  is introduced to depict the interaction strength [42]. Hereafter we are interested in the case of repulsive interaction. Inserting the BA wavefunction into Schrödinger equation and omitting the unwanted terms, one arrives at the Bethe ansatz equations (BAEs)

$$\lambda_j + \frac{1}{L} \sum_{k=1}^N \theta(\lambda_j - \lambda_k) = \frac{2\pi}{L} I_j, \quad j = 1, \dots, N \quad (2)$$

where  $\theta(x) = 2 \arctan(x/c)$ , pseudomomenta  $\{\lambda_j\}$  are distinct real numbers and quantum numbers (QNs)  $\{I_j\}$  are distinct integers (half-integers) if  $N$  is odd (even). There is a one-to-one map between a set of QNs and a set of pseudomomenta, by utilizing which the total momentum and energy of system are expressed as  $P_{\{\lambda\}} = \sum_{j=1}^N \lambda_j$ ,  $E_{\{\lambda\}} = \sum_{j=1}^N \lambda_j^2$ . The ground state is formulated by a Fermi sea-like distribution for QNs (i.e.  $I = \{-\frac{N-1}{2}, \dots, \frac{N-1}{2}\}$ ), and excited states can be obtained by generating pairs of particle-hole (p-h) over it.

We start from the single particle Green's function defined by

$$i \cdot \mathcal{G}(x, t) \equiv \langle \mathcal{T} [\Psi(x, t) \Psi^\dagger(0, 0)] \rangle_N \quad (3)$$

where  $\langle \dots \rangle_N$  means expectation value taken over the ground state of  $N$  particles, and  $\Psi(x, t)$  is bosonic

field operators in Heisenberg picture. For simplicity, hitherto we merely consider the larger Green's function  $G^>(x, t)$ , and treatment for the lesser case is similar. Inserting a completeness relation into the two field operators gives rise to  $i \cdot G^>(x, t) = \sum_{\{\mu\}_{N+1}} \frac{\langle \{\lambda\}_N | \Psi(x, t) | \{\mu\}_{N+1} \rangle \langle \{\mu\}_{N+1} | \Psi^\dagger(0, 0) | \{\lambda\}_N \rangle}{\langle \{\lambda\}_N | \{\lambda\}_N \rangle \langle \{\mu\}_{N+1} | \{\mu\}_{N+1} \rangle}$  where  $|\{\nu\}_M\rangle$  is an eigenstate consisting of  $M$  particles and specified by a set of pseudomomenta  $\{\nu\}_M$ . The ground state and excited state are respectively denoted as  $|\{\lambda\}_N\rangle$  and  $|\{\mu\}_{N+1}\rangle$ , see Supplementary Material [58]. Here the matrix elements of the field operators between two eigenstates present in the numerator are called *form factors*, which together with the norm square of eigenstates can be evaluated in terms of pseudomomenta by appealing to the algebraic Bethe ansatz method [45]. Based on these notations, we have

$$i \cdot G^>(x, t) = \sum_{\{\mu\}_{N+1}} e^{i\phi^+} \frac{|F(\{\lambda\}_N, \{\mu\}_{N+1})|^2}{\|\{\mu\}_{N+1}\|^2 \cdot \|\{\lambda\}_N\|^2} \quad (4)$$

with  $\phi^+ = (E_{\{\lambda\}} - E_{\{\mu\}})t - (P_{\{\lambda\}} - P_{\{\mu\}})x$ , and  $F(\{\alpha\}_M, \{\beta\}_{M+1})$  being an algebraic function of the two sets of pseudomomenta  $\{\alpha\}_M$  and  $\{\beta\}_{M+1}$  [58]. On basis of these results and the definition of SF  $A(k, \omega) = -\frac{1}{\pi} \text{Im} \mathcal{G}(k, \omega)$ , where  $\mathcal{G}(k, \omega)$  is the Fourier transform of  $\mathcal{G}(x, t)$ , one finally obtains

$$\begin{aligned} \frac{A(k, \omega)}{L} = & \sum_{\{\mu\}_{N+1}} \frac{\delta_{k, P_{\{\mu\}, \{\lambda\}}} \delta(\omega - E_{\{\mu\}, \{\lambda\}}) |F(\{\lambda\}_N, \{\mu\}_{N+1})|^2}{\|\{\mu\}_{N+1}\|^2 \cdot \|\{\lambda\}_N\|^2} \\ & + \sum_{\{\mu\}_{N-1}} \frac{\delta_{-k, P_{\{\mu\}, \{\lambda\}}} \delta(\omega + E_{\{\mu\}, \{\lambda\}}) |F(\{\mu\}_{N-1}, \{\lambda\}_N)|^2}{\|\{\mu\}_{N-1}\|^2 \cdot \|\{\lambda\}_N\|^2}, \end{aligned} \quad (5)$$

where  $\delta_{n,m}$  is Kronecker delta function and  $C_{\{\mu\},\{\lambda\}} \equiv C_{\{\mu\}} - C_{\{\lambda\}}$  if  $C = P$  or  $E$ .

In the above equations, the intermediate state  $|\{\mu\}_M\rangle$  can be achieved by creating pairs of p-h over the Fermi sea. The sum includes all states in the Hilbert space. However, such a counting whole Hilbert space is neither possible nor necessary in practice. In light of the different spectral weights of these states, here we compute the SF with high accuracy by considering the highly contributive states as many as possible. The key idea to realizing such possibility is to find suitable way to count in and classify all states [58]. Our algorithm is sketched as following. Owing to the nature of free quasiparticles, excitations with momentum  $k$  can be decomposed into numbers of p-h excitations. A given excited momentum  $k$  specifies an integer  $P_m = kL/2\pi$ , i.e. the total shift of QNs. Since a p-h excitation may occur rightward or leftward, we thus define the leftward shift  $P_l = 0, 1, 2, \dots$  and rightward shift  $P_r = P_l + P_m$ . If  $P_l = 0$ , all excitations are rightward, and then  $P_m$  is divided into a sum of  $N_p$  integers, corresponding to  $N_p$ -pairs of p-h. In the case of non-vanishing  $P_l$ , we define the number of leftward excitation  $N_l$ , and then  $P_l$  is divided into a sum of  $N_l$  integers and  $P_r$  into  $N_p - N_l$  integers, which respectively stand for  $N_l$  leftward and  $N_p - N_l$  rightward p-h excitations. Once such a tag of  $(P_m, N_p, P_l, N_l)$  is assigned, according to it we move the QNs and in consequence produce several excited states sharing the same tag [58]. We would like to emphasize that the whole Hilbert space can be navigated through the choice of different tags, and both  $N_p$  and  $P_l$  serve as a very convenient cut-off in our algorithm. The efficiency of this counting game is quantitatively checked by the saturation of SP,

$$\sum_k \int_{-\infty}^0 \frac{d\omega}{N} A(k, \omega) = 1. \quad (6)$$

*Results* — The logarithm of SF for Lieb-Liniger gas is demonstrated in Fig.1, resolved in momentum-energy. Here the focus is concentrated on the intermediate interaction region ( $\gamma = 4.0$ ) and weak interaction ( $\gamma = 0.5$ ) for sake of comparison. The yellow (black) dashed lines stand for the Lieb - I (- II) dispersion relations, corresponding to creation of a particle (hole) outside (inside) of Fermi sea. Single-particle and -hole excitations defining the edges of spectra feature the non-trivial role of interaction in 1D many-body systems. Fig.1 shows the SF of full momentum and energy scales for weak and strong interaction strengths. The energy of hole excitation is suppressed when the interaction strength  $\gamma$  decreases, but the Lieb - II dispersion exists as long as  $\gamma$  does not vanish. This feature makes the Bogoliubov approximation deficient and the explicit explanation was first put forward by the Bethe ansatz solution in this model [42]. The spectral weight distribution reveals the characteristic of particle-hole asymmetry in 1D, in addition to which the interaction apparently broadens the

$\delta$ -type peak on the threshold for SF of non-interacting bosons. It is obvious that either absorption or emission spectrum is separated into three regions all of that are determined by pairs of p-h excitations. Let us denote the Lieb - I (- II) dispersion as  $\epsilon_p$  ( $\epsilon_h$ ) in the particle sector  $\omega > 0$ , and as  $-\epsilon_p$  ( $-\epsilon_h$ ) in the hole sector  $\omega < 0$ . For the half plane of  $\omega > 0$ , below  $\epsilon_h$  is blank, implying no state bears the energy and momentum. For  $\epsilon_h < \omega < \epsilon_p$  a continuum spectrum consisting of states produced by arbitrary pairs of p-h excitations occurs, while for  $\omega > \epsilon_p$ , it is the regions where the excitations involve the excited states of 2-, 3-, and higher p-h pairs.

We show the curve of SF vs energy in Fig.2 with fixed momentum  $k = 0.1k_F$ , where  $\gamma = 4.0$ . We observe that a full capture of singular behaviour of the SF in the vicinities of the threshold requires the system size as large as  $N = L = 4000$ . The particle-hole asymmetry is evidenced in Fig.2a, where the blue (red) curve within absorption (emission) spectrum has a peak around the Lieb - II (- I) dispersion. The mechanism of their birth is distinct. The red peak mainly comes from the single p-h excitation while the blue one from multi-pairs of p-h excitation.

In Fig.2b the fascinating many-body phenomenon FES is observed, which is a typical impurity problem closely related to orthogonal catastrophe [1, 14]. The FES manifests that the SF on the thresholds of spectra displays power-law behavior [13, 15]

$$A(k, \omega) \sim \text{const} + |\omega \mp \epsilon_{p,h}|^{\mu_{\pm}}, \quad (7)$$

where subscript  $+$  ( $-$ ) stand for the edge exponent on absorption (emission) threshold. The original FES arises from the transient potential brought forth by a deep electron excitation, which leaves behind a core hole and scatters with the non-interacting electrons in conduction band [14]. It was interpreted as an impurity problem, i.e. an impurity moving in a Fermi liquid. By inclusion of interaction between particles, one reformed it as a Luttinger liquid instead [5]. However, the conventional TLL only identifies the power-law, the p-h symmetry of its own prevents from distinguishing four thresholds [1, 5]. This ambiguity disappears if we take into account of the nonlinearity in spectrum by combining the Bosonization and quantum integrable theory together [13]. In our method, the threshold behavior of SF in thermodynamic limit is directly observed as well. Using the log-log coordinates, the exponents represented by dashed lines are readily to obtain:  $\bar{\mu}_-$ ,  $\underline{\mu}_-$ ,  $\bar{\mu}_+$ , and  $\underline{\mu}_+$  are  $-0.465$ ,  $1.141$ ,  $-0.529$ , and  $0.977$ . Our results give the power-law behavior in good agreement with the edge exponents derived from nonlinear TLL, i.e.  $-0.422$ ,  $0.934$ ,  $-0.501$ , and  $1.043$  [13], confirming remarkably the nonlinear TLL. The observing FES of a large system size  $N = L = 4000$  shows the capability of our approach to dynamical correlations in high precision.

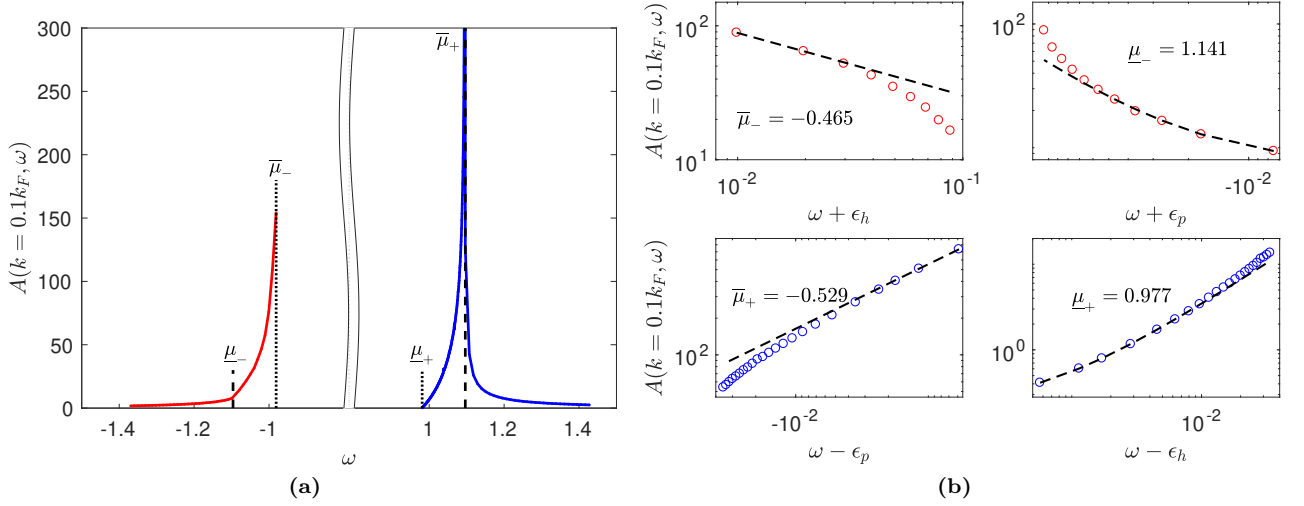


FIG. 2: SF vs energy given at a specified momentum  $k = 0.1k_F$  and intermediate interaction strength  $\gamma = 4.0$ . The system size is  $N = L = 4000$ , and energy is given in unit of Fermi energy. (a) shows the full feature of the SF along with energy where red (blue) curve is for emission (absorption) spectrum, and black dashed (dotted) lines are the thresholds of single particle spectrum  $\pm\epsilon_p$  ( $\pm\epsilon_h$ ). Apparently, there exists a peak around Lieb - I (- II) dispersion in absorption (emission) spectrum. Between the two Lieb - II excitations is blank in Fig.1. (b) shows the singular powers of SF in the vicinities of the thresholds of single-particle spectrum. A log-log coordinate is used for clear visibility. The red (blue) circles represent SF in emission (absorption) spectrum and black dashed lines are the asymptotic gradients. The extracted exponents  $\bar{\mu}_-$ ,  $\mu_-$ ,  $\bar{\mu}_+$ , and  $\mu_+$  are  $-0.465$ ,  $1.141$ ,  $-0.529$ , and  $0.977$ , which agree well with the prediction based on nonlinear TLL  $-0.422$ ,  $0.934$ ,  $-0.501$ , and  $1.043$ , respectively.

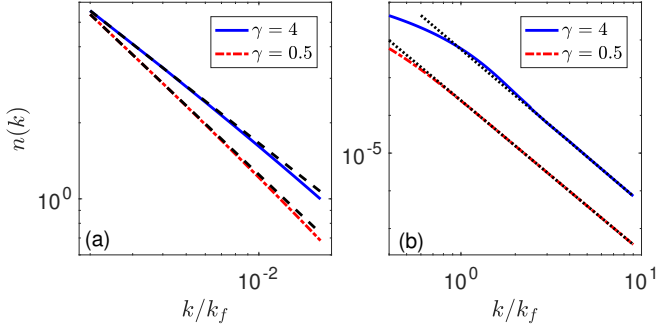


FIG. 3: (a) The momentum distribution in the small momentum region. The black dashed lines represent the asymptotic powers when  $k \rightarrow 0$ , with  $-0.750$  and  $-0.908$  for  $\gamma = 4$  and  $0.5$  respectively. They agree with the TLL predictions  $-0.737$  and  $-0.894$ , here we set  $N = L = 1000$  for our numerical calculation. (b) The momentum distributions for  $\gamma = 0.5$  and  $4$ , respectively. The gradients of black dotted lines show the asymptotic powers for a large momentum,  $-4.073$  and  $-4.001$  for  $\gamma = 4$  and  $0.5$  respectively. They agree well with power-law for the momentum tail  $k^{-4}$ . The system size is set as  $N = L = 100$  for this plot.

Last but not least, we study the power-law behavior of momentum distribution, i.e. static correlation function  $n(k) = \int_{-\infty}^0 \frac{d\omega}{2\pi L} A(k, \omega)$  in Fig.3. For the tail part of momentum distribution, see Fig.3 (b), where the system size is  $N = L = 100$ , the same as Fig.1. The exponents are extracted by the black dotted lines, with the gradients  $-4.00$  and  $-4.07$  for  $\gamma = 0.5$  and  $4$  respectively. It is ob-

viously that they are in good agreement with theoretical predication  $\lim_{k \rightarrow \infty} n(k) \sim k^{-4}$ . For the small momentum region, see Fig.3 (a), the data of Fig.1 are not enough due to finite-size effect. We therefore make use of data of a large system  $N = L = 1000$ . The gradients of black dashed lines are  $-0.750$  and  $-0.908$  for  $\gamma = 4$  and  $0.5$  respectively. According to TLL,  $\lim_{k \rightarrow 0} n(k) \sim k^{1/2K-1}$  [1], and easy calculation gives the powers  $-0.737$  and  $-0.894$ , showing a good agreement with our exact numerical results. This indicates a high capability of our approach to the critical behaviour of correlation functions in thermodynamic limit. By now, one may have an empirical estimation regarding the system size which helps with capturing singular behaviour of the correlation functions in thermodynamic limit: for the static one, tens to hundreds are needed, while for the dynamic one, thousands at least.

*Conclusion* — The method for exactly computing the SF and momentum distribution of Lieb-Liniger gas has been reported by the virtue of algebraic Bethe ansatz, form factor and numerics. For an arbitrary interaction within a large system, the precise Fermi edge singularities has been given explicitly that essentially confirms the nonlinear TLL. We have observed that in order to capture the full threshold singular behavior, a large system size ( $N = 4000$ ) is requested. Moreover, we have obtained the power-law of momentum distribution in large and small momentum region, showing an excellent agreement with the theoretical prediction. This work provides



a reliable approach to various features of correlation functions in thermodynamic limit, and complements the previous studies on Lieb-Liniger model [54, 56] and other 1D bosonic system in the TG limit [33, 34]. Besides, our method can be generalized to other quantum integral models as well.

*Acknowledgments.* SC and YYC contributed equally to this paper. SC is grateful to Andrea Trombettoni and Feng He for their helpful discussions. This work is supported by National Natural Science Foundation of China Grants Nos. 12104372, 12047511, 12047502, 12134015, 11874393 and 12121004. SC, RM and HQL acknowledge the computational resources from the Beijing Computational Science Research Center.

---

\* chenyy@nwnu.edu.cn

† haiqing0@csrc.ac.cn

- [1] T. Giamarchi, *Quantum Physics in One Dimension* (Oxford University Press, Oxford, 2004).
- [2] L. D. Landau, Sov. Phys. JETP, **3** 920 (1957); *ibid.* **5**, 101 (1957).
- [3] Gordon Baym and Christopher Pethick, *Landau Fermi-liquid theory: concepts and applications*, (John Wiley & Sons, 2008).
- [4] Philip W. Anderson, and F. Duncan M. Haldane, J. Stat. Phys. **103**, 425 (2001).
- [5] Alexander O. Gogolin, Alexander A. Nersisyan, and Alexi M. Tsvelik, *Bosonization and Strongly Correlated Systems* (Cambridge University Press, Cambridge, 1998).
- [6] M. A. Cazalilla, R. Citro, T. Giamarchi, E. Orignac, and M. Rigol, Rev. Mod. Phys. **83**, 1405 (2011); M. A. Cazalilla, J. Phys. B **37**, S1 (2004).
- [7] Adilet Imambekov, Thomas L. Schmidt and Leonid I. Glazman, Rev. Mod. Phys. **84**, 1253 (2012).
- [8] Xi-Wen Guan, Murray T. Batchelor, and ChaoHong Lee, Rev. Mod. Phys. **85**, 1633 (2013).
- [9] X.-B. Zhang, et. al. Science **335**, 1070 (2012).
- [10] B. Yang, Y.-Y. Chen, Y.-G. Zheng, H. Sun, H.-N. Dai, X.-W. Guan, Z.-S. Yuan and J.-W. Pan, Phys. Rev. Lett. **119**, 165701 (2017).
- [11] X.-B. Zhang, Y.-Y. Chen, L.-X. Liu, Y.-J. Deng and X.-W. Guan Natl. Sci. Rev., <https://doi.org/10.1093/nsr/nwac027>.
- [12] Till D. Kühner, Steven R. White, and H. Monien, Phys. Rev. B **61**, 12474 (2000).
- [13] Adilet Imambekov, and Leonid I. Glazman, Phys. Rev. Lett. **100**, 206805 (2008).
- [14] Gerald D. Mathan, *Many-Particle Physics* (Springer, New York, 2000).
- [15] M. Pustilnik, M. Khodas, A. Kamenev, L. Glazman, Phys. Rev. Lett. **96**, 196405 (2006).
- [16] Adilet Imambekov, and Leonid I. Glazman, Science **323**, 228 (2009).
- [17] Adilet Imambekov, and Leonid I. Glazman, Phys. Rev. Lett. **102**, 126405 (2009).
- [18] Thomas L. Schmidt, Adilet Imambekov, and Leonid I. Glazman, Phys. Rev. Lett. **104**, 116403 (2010).
- [19] N. Kitanine, K. K. Kozłowski, J. M. Maillet, N. A. Slavnov, and V. Terras, J. Stat. Mech. P09001 (2012).
- [20] Belén Paredes, Artur Widera, Valentin Murg, Olaf Mandel, Simon Fölling, Ignacio Cirac, Gora V. Shlyapnikov, Theodor W. Hänsch, Immanuel Bloch, Nature **429**, 277 (2004).
- [21] J. T. Stewart, J. P. Gaebler, D. S. Jin, Nature **454**, 744 (2008); A. Bohrdt, D. Greif, E. Demler, M. Knap, and F. Grusdt, Phys. Rev. B **97**, 125117 (2018).
- [22] Tung-Lam Dao, Antoine Georges, Jean Dalibard, Christophe Salomon, and Iacopo Carusotto, Phys. Rev. Lett. **98**, 240402 (2007); Dao Tung-Lam, Carusotto Iacopo, and Georges Antoine, Phys. Rev. A **80**, 023627 (2009).
- [23] G. Veeravalli, E. Kuhnle, P. Dyke, C. J. Vale, Phys. Rev. Lett. **101**, 250403 (2008).
- [24] N. Fabbri, M. Panfil, D. Clément, L. Fallani, M. Inguscio, C. Fort, and J.-S. Caux, Phys. Rev. A **91**, 043617 (2015).
- [25] R. Senaratne, D. Cavazos-Cavazos, S. Wang, F. He, Y.-T. Chang, A. Kafle, H. Pu, X.-W. Guan and R. G. Hulet, Science **376**, 1305 (2022).
- [26] M. Girardeau, J. Math. Phys. **1**, 516 (1960); Phys. Rev. **139** B500 (1965).
- [27] A. Lenard, J. Math. Phys. **5**, 930 (1964), *ibid.* **7**, 1268 (1966).
- [28] H. G. Vaidya, and C. A. Tracy, Phys. Rev. Lett. **42**, 3 (1979); J. Math. Phys. **20**, 2291 (1979).
- [29] V. E. Korepin and N. A. Slavnov, Commun. Math. Phys. **129**, 103 (1990).
- [30] E. Granet, J. Phys. A: Math. Theor. **54**, 154001 (2021).
- [31] E. Granet, F. H. L. Essler, SciPost Phys. **9**, 082 (2020).
- [32] F. Meinert, M. Panfil, M. J. Mark, K. Lauber, J.-S. Caux and H. C. Nägerl Phys. Rev. Lett. **115**, 085301 (2015).
- [33] R. Pezer, and H. Buljan, Phys. Rev. Lett. **98**, 240403 (2007).
- [34] J. Settino, N. Lo Gullo, F. Plastina, and A. Minguzzi, Phys. Rev. Lett. **126**, 065301 (2021).
- [35] V. V. Cheianov, H. Smith and M. B. Zvonarev, J. Stat. Mech.: Theory and Experiment, P08015 (2006); Phys. Rev. A **73**, 051604(R) (2006).
- [36] E. K. J. P. Nandani, R. Römer, S. Tan and X.-W. Guan, New J. Phys. **18**, 055014 (2016).
- [37] M. Kormos, G. Mussardo, and A. Trombettoni, Phys. Rev. Lett. **103**, 210404 (2009).
- [38] M. Kormos, Y.-Z. Chou, A. Imambekov, Phys. Rev. Lett. **107**, 230405 (2011).
- [39] K. V. Kheruntsyan, D. M. Gangardt, P. D. Drummond, and G. V. Shlyapnikov, Phys. Rev. Lett. **91**, 040403 (2003).
- [40] D. M. Gangardt and G. V. Shlyapnikov, Phys. Rev. Lett. **90**, 010401 (2003); New. J. Phys. **5**, 79 (2003).
- [41] F. D. M. Haldane, Phys. Rev. Lett. **47**, 1840 (1981); J. Phys. C **14**, 2589 (1981).
- [42] E. H. Lieb, and W. Liniger, Phys. Rev. **130**, 1605 (1963); E. H. Lieb, *ibid.* **130**, 1616 (1963).
- [43] Jiang Yu-Zhu, Chen Yang-Yang, and Guan Xi-Wen, Chin. Phys. B **24**, 050311 (2015).
- [44] Fabio Franchini, *An Introduction to Integrable Techniques for One-Dimensional Quantum Systems* (Springer, Cham, 2017).
- [45] V. E. Korepin, N. M. Bogoliubov, and A. G. Izergin, *Quantum Inverse Scattering Method and Correlation Functions* (Cambridge University Press, Cambridge, 1993).

- [46] X.-W. Guan, and P. He, Rep. Prog. Phys., *accepted*, 2022.
- [47] V. E. Korepin, and N. A. Slavnov, Commun. Math. Phys. **136**, 633 (1991).
- [48] T. Kojima, V. E. Korepin, and N. A. Slavnov, Commun. Math. Phys. **188**, 657 (1997).
- [49] T. Kojima, V. E. Korepin, and N. A. Slavnov, Commun. Math. Phys. **189**, 709 (1997).
- [50] A. R. Its, and N. A. Slavnov, Teor. Mat. Fiz. **119**, 179 (1999); N. A. Slavnov Teor. Mat. Fiz. **121**, 117 (1999).
- [51] V. E. Korepin, Commun. Math. Phys. **86**, 391 (1982).
- [52] V. E. Korepin, Commun. Math. Phys. **94**, 93 (1984).
- [53] N. A. Slavnov, Teor. Mat. Fiz. **79**, 232 (1989); *ibid.* **82**, 389 (1990).
- [54] Jean-Sébastien Caux, and Pasquale Calabrese, Phys. Rev. A **74**, 031605(R) (2006).
- [55] Milosz Panfil, and Jean-Sébastien Caux, Phys. Rev. A **89**, 033605 (2014).
- [56] Jean-Sébastien Caux, and Pasquale Calabrese, and Nikita A. Slavnov, J. Stat. Mech. (2007) P01008.
- [57] Song Cheng, Yangyang Chen, Xiwen Guan, Wenli Yang, Rubem Mondaini, and Haiqing Lin, *not published*.
- [58] All the invovled representations are listed in Supplement Material.

## Supplementary Material for The Exact Spectral Function of One-Dimensional Bose Gases

Song Cheng, Yang-Yang Chen,\* Xi-Wen Guan, Wen-Li Yang, Rubem Mondaini, and Hai-Qing Lin†  
(Dated: September 30, 2022)

### THE DETERMINANT REPRESENTATIONS OF FORM FACTORS

We list the main results of form factors present in the article, and recommend Refs. [1–4] for those who are interested in derivations in detail. In particular, Ref. [1] offers a pedagogical access to the algebraic Bethe ansatz technique and the various methods in calculating correlated properties of quantum integrable models.

If  $\{k\}_M$  satisfies the BA equations, then the norm square of eigenvector  $|\{k\}_M\rangle$  is expressed by

$$\|\{k\}_M\|^2 \equiv \langle\{k\}_M|\{k\}_M\rangle = c^M \prod_{j>l\geq 1}^M \frac{k_{jl}^2 + c^2}{k_{jl}^2} \det_M \mathfrak{G}(\{k\}_M) \quad (1)$$

where  $\mathfrak{G}(\{k\}_M)$  is the Gaudin matrix with entry

$$\mathfrak{G}_{jl}(\{k\}_M) = \delta_{jl} \left[ L + \sum_{s=1}^M K(k_j, k_s) \right] - K(k_j, k_l) \quad (2)$$

and kernel function

$$K(x, y) = \frac{2c}{(x - y)^2 + c^2}. \quad (3)$$

The norm square for  $F(\{\lambda\}_N, \{\mu\}_{N+1})$  is

$$\|F(\{\lambda\}_N, \{\mu\}_{N+1})\|^2 = c^{2N+1} \frac{\prod_{j>k\geq 1}^{N+1} (\mu_{jk}^2 + c^2)^2}{\prod_{a=1}^{N+1} \prod_{b=1}^N (\mu_a - \lambda_b)^2} (\det_N U(\{\lambda\}_N, \{\mu\}_{N+1}))^2, \quad (4)$$

where the  $N \times N$  matrix  $U(\{\lambda\}_N, \{\mu\}_{N+1})$  is a function of two sets of pseudomomenta

$$U_{jk}(\{\lambda\}_N, \{\mu\}_{N+1}) = \delta_{jk} \cdot (V_j^+ - V_j^-) / i + \frac{\prod_{a=1}^N (\lambda_a - \mu_j)}{\prod_{a \neq j}^{N+1} (\mu_a - \mu_j)} (K(\mu_j - \mu_k) - K(\mu_N - \mu_k)), \quad (5)$$

$$V_j^\pm = \frac{\prod_{a=1}^N (\lambda_a - \mu_j \pm ic)}{\prod_{a=1}^{N+1} (\mu_a - \mu_j \pm ic)}. \quad (6)$$

### EXPONENTS OF EDGE SINGULARITY

The exact exponents of edge singularity for spectral function of Lieb-Liniger model was firstly calculated by a combination of nonlinear TLL theory and quantum integrability [5]. In order to obtain the exponents, one needs to solve two integral equations. One is for the shift function [1]

$$F_B(\nu|\lambda) = \frac{\pi + \theta(\nu - \lambda)}{2\pi} + \frac{1}{2\pi} \int_{-q}^q d\mu K(\nu, \mu) F_B(\mu|\lambda) \quad (7)$$

where  $\theta(x) = 2 \arctan(x/c)$  and  $K(x, y)$  is defined by Eq. (3). Note that  $q > 0$  is the cut-off of pseudomomentum for ground state in thermodynamic limit. The other one is for the change of total momentum when adding a particle (hole) with pseudomomentum  $\lambda > q$  ( $|\lambda| < q$ ) to the ground state. This change  $k(\lambda)$  is expressed by

$$k(\lambda) = \pm \left( \lambda - \pi n + \int_{-q}^q d\nu \theta(\lambda - \nu) \rho(\nu) \right) \quad (8)$$

where  $\pm$  is to specify adding a particle or hole and  $\rho(x)$  is the distribution of pseudomomenta in thermodynamic limit, governed by following integral equation

$$\rho(\lambda) = \frac{1}{2\pi} + \frac{1}{2\pi} \int_{-q}^q d\mu K(\lambda, \mu) \rho(\mu). \quad (9)$$

These exponents therefore read

$$\bar{\mu}_{\pm} = \frac{1}{2} \left( \frac{\delta_{+} - \delta_{-}}{2\pi} \right)^2 + \frac{1}{2} \left( \frac{\delta_{+} + \delta_{-}}{2\pi} \right)^2 - 1, \quad (10)$$

$$\underline{\mu}_{\pm} = \frac{1}{2} \left( \frac{2}{\sqrt{K}} + \frac{\delta_{+} - \delta_{-}}{2\pi} \right)^2 + \frac{1}{2} \left( \frac{\delta_{+} + \delta_{-}}{2\pi} \right)^2 - 1 \quad (11)$$

where  $\delta_{\pm} = 2\pi F_B(\pm q, \lambda)$  and  $K$  is the Luttinger parameter.

By taking  $\bar{\mu}_{+}$  ( $\underline{\mu}_{+}$ ) as an example, we outline the numerical treatment for above integral equations. As  $\bar{\mu}_{+}$  ( $\underline{\mu}_{+}$ ) lies on the threshold generated by adding 1-particle ( 2-particles close to the same Fermi point and 1-hole) to the ground state, the sign in Eq. (8) is positive (negative). One should solve the corresponding  $\lambda$  by using Eq. (8), and then substitute this  $\lambda$  into the shift function  $F_B(\pm q|\lambda)$ . With the help of Eq. (7),  $\delta_{\pm}(k)$  and thus the exponent  $\bar{\mu}_{+}$  ( $\underline{\mu}_{+}$ ) is obtained.

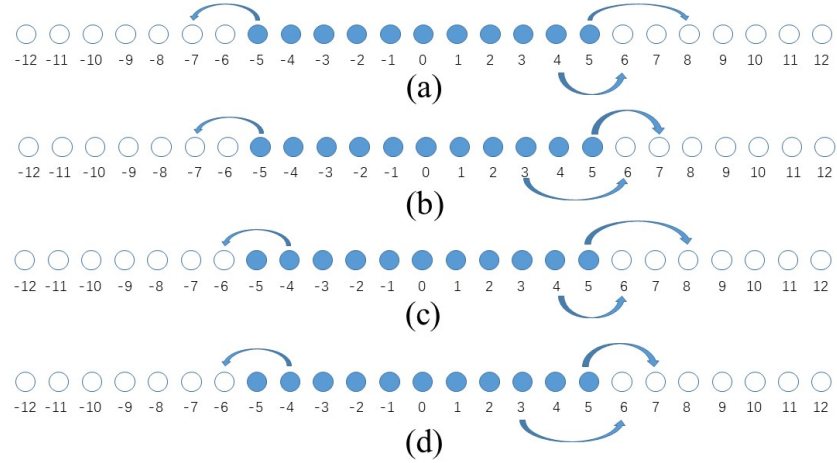


FIG. 1. A sketch to display the excited states sharing the same tag  $P_m = 3$ ,  $N_p = 3$ ,  $P_l = 2$ ,  $N_l = 1$ . The system size is  $N = 11$ . We use balls and circles to stand for particles and holes respectively, and arrows to explain the movement of particles. The excitation generates states listed as below, (a):  $\{-7, -4, -3, -2, -1, 0, 1, 2, 3, 6, 8\}$ , (b):  $\{-7, -4, -3, -2, -1, 0, 1, 2, 4, 6, 7\}$ , (c):  $\{-6, -5, -3, -2, -1, 0, 1, 2, 3, 6, 8\}$ , (d):  $\{-6, -5, -3, -2, -1, 0, 1, 2, 4, 6, 7\}$ .

### AN EXAMPLE: HOW TO COUNT THE STATES

Here we give an explicit example to show how the algorithm works.

At first, we show the way to produce excited states sharing the same tag in Figure 1. The system consists of  $N = 11$  particles and we set  $N_p = 3$ ,  $P_m = 3$ ,  $P_l = 2$ ,  $N_l = 1$ , without losing generality. As is described in the main text, the ground state is a line of continuous integers from  $-5$  to  $5$ . This tag set means 3 particles jumping outside of Fermi sea, 2 rightward and 1 leftward. The total shift of quantum numbers is  $P_m = 3$ , and  $P_r = 5$  &  $P_l = 2$ . The integers are the available quantum numbers (QNs), and the blue ball (circle) represents the corresponding QN is occupied (vacant) alias a particle (hole). The arrows is applied to specify the movement of particles in this excitation. There



Tags				Sum Rule			
$P_m$	$N_p$	$P_l$	$N_l$	$N_l$ -sum rule	$P_l$ -sum rule	$N_p$ -sum rule	$P_m$ -sum rule
10	1	0	0	0.0101	0.0101	0.0101	0.0140
		2	0	$2.1387 \times 10^{-4}$	$2.1387 \times 10^{-4}$	0.0038	
			1	0.0013	0.0013		
		2	1	$6.7836 \times 10^{-4}$	$6.7836 \times 10^{-4}$		
		3	1	$4.3148 \times 10^{-4}$	$4.3148 \times 10^{-4}$		
		4	1	$3.0257 \times 10^{-4}$	$3.0257 \times 10^{-4}$		
		5	1	$2.2441 \times 10^{-4}$	$2.2441 \times 10^{-4}$		
		6	1	$1.7271 \times 10^{-4}$	$1.7271 \times 10^{-4}$		
		7	1	$1.3648 \times 10^{-4}$	$1.3648 \times 10^{-4}$		
		8	1	$1.1002 \times 10^{-4}$	$1.1002 \times 10^{-4}$		
	2	9	1	$9.0073 \times 10^{-5}$	$9.0073 \times 10^{-5}$		
		10	1	$7.4669 \times 10^{-5}$	$7.4669 \times 10^{-5}$		
		$\vdots$	$\vdots$	$\vdots$	$\vdots$		
		$\vdots$	$\vdots$	$\vdots$	$\vdots$		
		3	0	$4.4310 \times 10^{-10}$	$4.4310 \times 10^{-10}$	$1.1479 \times 10^{-4}$	
			1	$3.2147 \times 10^{-5}$	$3.2147 \times 10^{-5}$		
		2	1	$1.8195 \times 10^{-5}$	$1.8195 \times 10^{-5}$		
			1	N/A	N/A		
		4	1	$9.6819 \times 10^{-6}$	$1.0361 \times 10^{-5}$		
			2	$6.7925 \times 10^{-7}$			
	3	5	1	$7.7140 \times 10^{-6}$	$8.9681 \times 10^{-6}$		
			2	$1.2541 \times 10^{-6}$			
		6	1	$6.3243 \times 10^{-6}$	$7.9483 \times 10^{-6}$		
			2	$1.6240 \times 10^{-6}$			
		7	1	$5.2867 \times 10^{-6}$	$7.1125 \times 10^{-6}$		
			2	$1.8258 \times 10^{-6}$			
		8	1	$4.4816 \times 10^{-6}$	$6.3910 \times 10^{-6}$		
			2	$1.9094 \times 10^{-6}$			
		9	1	$3.8394 \times 10^{-6}$	$5.7539 \times 10^{-6}$		
			2	$1.9145 \times 10^{-6}$			
	10	1	1	$3.3162 \times 10^{-6}$	$5.1856 \times 10^{-6}$		
			2	$1.8695 \times 10^{-6}$			
		$\vdots$	$\vdots$	$\vdots$	$\vdots$		
		$\vdots$	$\vdots$	$\vdots$	$\vdots$		

TABLE I. An example for the hole sector of spectral function with given excited momentum  $k = 0.2k_F$  of system size  $N = L = 100$  and interaction strength  $\gamma = 4$ . The  $X$ -sum rule is the total spectral weights of the states under tag  $X$ , such as  $N_p$ -sum rule specifying the contribution of different pairs of p-h excitation. Here N/A means there is no state under that tag.

is one particle jumping leftward out of Fermi sea with step length  $P_l = 2$ . It is obvious that there are merely two possible arrangements for this leftward excitation, realized by moving either of the two neighbors (QNs  $-5$  or  $-4$ ) of left Fermi point. For the rightward excitation, the situation is a little bit different, the simultaneous movement of two QNs with total shift  $P_r = 5$ . The step length of each movement should be 2 or 3, and the case of 4 and 1 is ruled out because it will generate repeated states belonging to other tags.

Following the production of excited states, Table I displays the data of one-body dynamical correlation function (the hole sector of spectral function  $\omega < 0$ ) at a given excited momentum. The system size is  $N = L = 100$ , interaction strength is  $\gamma = 4$ , and the excited momentum is  $k = 0.2k_F$ . According to the introduction of algorithm in main text,  $P_m = 10$ ,  $N_p = 1, 2, 3$ , and  $P_l = 0, 1, 2, \dots, 10$ . Note that N/A is exactly the case discussed before that repeated states belonging to other tags. Obviously the results show both  $N_p$  and  $P_l$  serve as good criteria for cut-off.

\* chenyy@nwu.edu.cn

† haiqing0@csrc.ac.cn

- [1] V. E. Korepin, N. M. Bogoliubov, and A. G. Izergin, *Quantum Inverse Scattering Method and Correlation Functions* (Cambridge University Press, Cambridge, 1993).
- [2] T. Kojima, V. E. Korepin, and N. A. Slavnov, Commun. Math. Phys. **188**, 657 (1997).
- [3] T. Kojima, V. E. Korepin, and N. A. Slavnov, Commun. Math. Phys. **189**, 709 (1997).

- [4] Jean-Sébastien Caux, and Pasquale Calabrese, and Nikita A. Slavnov, J. Stat. Mech. (2007) P01008.
- [5] Adilet Imambekov, and Leonid I. Glazman, Phys. Rev. Lett. **100**, 206805 (2008).